Sum rules and physical bounds on passive metamaterials

Gustafsson, Mats; Sjöberg, Daniel

2010

CODEN:LUTEDX/(TEAT-7186)/1-19/(2010)

Sum rules and physical bounds on passive metamaterials

Mats Gustafsson and Daniel Sjöberg

Electromagnetic Theory
Department of Electrical and Information Technology
Lund University
Sweden

Mats Gustafsson and Daniel Sjöberg
Mats.Gustafsson@eit.lth.se, Daniel.Sjoberg@eit.lth.se

Department of Electrical and Information Technology
Electromagnetic Theory
Lund University
P.O. Box 118
SE-221 00 Lund
Sweden

Editor: Gerhard Kristensson

Abstract

Frequency dependence of the permittivity and permeability is inevitable in metamaterial applications such as cloaking and perfect lenses. In this paper, Herglotz functions are used as a tool to construct sum rules from which we derive physical bounds suited for metamaterial applications, where the material parameters are often designed to be negative or near zero in the frequency band of interest. Several sum rules are presented that relate the temporal dispersion of the material parameters with the difference between the static and instantaneous parameter values, which are used to give upper bounds on the bandwidth of the application. This substantially advances the understanding of the behavior of metamaterials with extraordinary material parameters, and reveals a beautiful connection between properties in the design band (finite frequencies) and the low- and high-frequency limit.

1 Introduction

The intriguing physics based on negative index of refraction [28] and ϵ-near-zero materials [26] with applications such as the perfect lens [33] and cloaking [2, 24] has created a renewed interest in the fundamental properties of the interaction between electromagnetic fields and materials [14, 20, 32]. The ideal behavior of, *e.g.*, the (relative) permittivity is that $\epsilon(\omega) \approx \epsilon_{\rm m}$ over a range of angular frequencies, where $\epsilon_{\rm m}$ is a real-valued number, *e.g.*, $\epsilon_{\rm m} \approx -1$ or $\epsilon_{\rm m} \approx 0$, depending on the application [2, 26, 28, 33]. It is well known that the electromagnetic response of materials is temporally dispersive, *i.e.*, it depends on frequency. The classical Kramers-Kronig relations [10, 13, 16] relate the frequency dependence of the real- and imaginary parts of the permittivity and the permeability for causal material models.

In metamaterial applications it is essential to consider realistic material models to obtain reliable and physically realizable results. Since engineered materials with very complex frequency dependence are often considered, it is not sufficient to analyze only Drude and Lorentz models if all potentials and restrictions of future metamaterials applications are to be evaluated.

Approaches based on the Hilbert transform or equivalently the Kramers-Kronig relations [10] are commonly used to derive bounds for causal material models. The investigation in [32] is one attempt to understand the constraints that causality puts on negative index of refraction materials. However, as illustrated in [18], it is difficult to derive absolute bounds from this approach due to the high sensitivity to losses at the evaluation frequency [14]. In [20, 27], it is also shown that there are no severe restrictions if just the condition of causality is employed. The results in [17] show that $|\epsilon(\omega) - \epsilon_{\rm m}| \geq B$, where $\epsilon_{\rm m} = -1$ and B denotes the fractional bandwidth, if the additional assumption of passivity is used [13, 34]

In this paper, constraints on the constitutive relations based on the assumptions of causality and passivity are further analyzed. The analysis is for simplicity restricted to isotropic constitutive relations (with some extensions to bi-anisotropic media given in Sec. 4), that are characterized by their (relative) permittivity ϵ and (relative) permeability μ. The results are given in Sec. 3 as several sum rules that relate the instantaneous and static response of the material model with weighted integrals of the constitutive parameter over all spectrum. The integrals typically measure how close a material parameter $\epsilon(\omega)$ can be to a target value $\epsilon_{\rm m}$ over a frequency interval. The sum rules can be expressed as bounds on the variation around the target value, and are somewhat different depending on the value of $\epsilon_{\rm m}$. Let $\epsilon_{\rm s}$ and ϵ_∞ denote the limiting values of $\epsilon(\omega)$ as $\omega\to 0$ and $\omega\to\infty$, respectively. If $\epsilon_\infty\leq\epsilon_{\rm m}\leq\epsilon_{\rm s}$, there is in principle no bandwidth limitation, but if $\epsilon_{\rm m}<\epsilon_\infty$, we derive the following bounds in sections 3.1 and 3.2 (where $\mathcal{B}=[\omega_1,\omega_2]$ is the frequency band, and $B=(\omega_2-\omega_1)/\omega_0$ is the fractional bandwidth, writing $\omega_0=(\omega_2+\omega_1)/2$ for the center frequency):

$$\max_{\omega\in\mathcal{B}}|\epsilon(\omega)-\epsilon_{\rm m}|\geq\frac{B/2}{1+B/2}(\epsilon_\infty-\epsilon_{\rm m})\quad\text{(with or without static conductivity)}\tag{1.1}$$

$$\max_{\omega\in\mathcal{B}}\frac{|\epsilon(\omega)-\epsilon_{\rm m}|}{|\epsilon(\omega)-\epsilon_\infty|}\geq\frac{B/2}{1+B/2}\frac{\epsilon_{\rm s}-\epsilon_{\rm m}}{\epsilon_{\rm s}-\epsilon_\infty}\quad\text{(no static conductivity, \textit{i.e.}, an insulator)}\tag{1.2}$$

If instead the target value is larger than the static value, *i.e.*, $\epsilon_{\rm m}\geq\epsilon_{\rm s}$, we derive the following bound in Sec. 3.3:

$$\max_{\omega\in\mathcal{B}}\frac{|\epsilon(\omega)-\epsilon_{\rm m}|}{|\epsilon(\omega)-\epsilon_\infty|}\geq\frac{B/2}{1+B/2}\frac{\epsilon_{\rm m}-\epsilon_{\rm s}}{\epsilon_{\rm s}-\epsilon_\infty}\tag{1.3}$$

If the material is lossless in the frequency band of interest $\mathcal{B}=[\omega_1,\omega_2]$, the right hand sides should be multiplied by 2. The bounds can be tightened if *a priori* knowledge of the plasma frequency is added, see Sec. 3.4.

2 Theoretical background

2.1 Constitutive relations and Herglotz functions

We assume that the Maxwell equations in the time-domain can be used to model the interaction between the electromagnetic field and the material. The linear, causal, time translational invariant, continuous, and isotropic constitutive relations are [12]

$$\boldsymbol{D}(t)=\epsilon_0\epsilon_\infty\boldsymbol{E}(t)+\epsilon_0\int_{\mathbb{R}}\chi_{\rm ee}(t-t')\boldsymbol{E}(t')\,{\rm d}t'\tag{2.1}$$

and

$$\boldsymbol{B}(t)=\mu_0\mu_\infty\boldsymbol{H}(t)+\mu_0\int_{\mathbb{R}}\chi_{\rm mm}(t-t')\boldsymbol{H}(t')\,{\rm d}t',\tag{2.2}$$

where $\boldsymbol{\chi}_{\rm ee}(t)=0$ and $\boldsymbol{\chi}_{\rm mm}(t)=0$ for $t<0$, the dependence of the spatial coordinates is suppressed, and ϵ_0 and μ_0 denote the free space permittivity and permeability, respectively. The material model is passive if

$$0\leq\int_{-\infty}^{T}\boldsymbol{E}(t)\cdot\frac{\partial\boldsymbol{D}(t)}{\partial t}\,{\rm d}t=\epsilon_0\int_{-\infty}^{T}\int_{\mathbb{R}}\boldsymbol{E}(t)\cdot\frac{\partial}{\partial t}\big(\epsilon_\infty\delta(t-t')+\chi_{\rm ee}(t-t')\big)\boldsymbol{E}(t')\,{\rm d}t'\,{\rm d}t\tag{2.3}$$

and

$$0 \leq \int_{-\infty}^{T} \boldsymbol{H}(t)\cdot\frac{\partial \boldsymbol{B}(t)}{\partial t}\,\mathrm{d}t = \mu_0\int_{-\infty}^{T}\int_{\mathbb{R}} \boldsymbol{H}(t)\cdot\frac{\partial}{\partial t}\big(\mu_\infty\delta(t-t')+\chi_{\mathrm{mm}}(t-t')\big)\boldsymbol{H}(t')\,\mathrm{d}t'\,\mathrm{d}t \tag{2.4}$$

for all times T and fields $\boldsymbol{E}$ and $\boldsymbol{H}$. This classifies

$$\frac{\partial}{\partial t}\big(\epsilon_\infty\delta(t)+\chi_{\mathrm{ee}}(t)\big) \quad \text{and} \quad \frac{\partial}{\partial t}\big(\mu_\infty\delta(t)+\chi_{\mathrm{mm}}(t)\big) \tag{2.5}$$

as a passive convolution kernel [34], where $\delta(t)$ is the Dirac delta distribution. It also restricts the instantaneous responses ϵ_∞ and μ_∞ to be non-negative. Moreover, the Maxwell equations together with the constitutive relations (2.1) and (2.2) and standard initial and boundary conditions are well posed if $\epsilon_\infty > \alpha$ and $\mu_\infty > \alpha$ for some $\alpha > 0$. This means that this requirement is sufficient to guarantee that a solution exists, is unique, and depends continuously on data [15]. This is *e.g.*, required for numerical solutions in the time domain such as with finite differences [15]. Here, we analyze the constraints that passivity (2.3) and (2.4) enforces on the temporal dispersion of the models (2.1) and (2.2).

The wave-front speed limits the speed of the electromagnetic waves and is given by c_0/n_∞, where $n_\infty = \sqrt{\epsilon_\infty\mu_\infty}$ is the instantaneous refractive index. It is often assumed that materials reduce to free space in the high-frequency limit, implying that $n_\infty = \epsilon_\infty = \mu_\infty = 1$. This is possible, but it is not necessary for the results presented in this paper. Moreover, it is not obvious that $\epsilon_\infty = \mu_\infty = 1$ apply for all engineered materials. Instead, a modeling approach is used where the high-frequency limit is obtained by analytic continuation from the frequency interval of interest [7].

The Fourier transform (using time dependence $\mathrm{e}^{-\mathrm{i}\omega t}$) of the constitutive relations (2.1) and (2.2) gives the frequency domain model

$$\boldsymbol{D}(\omega) = \epsilon_0\epsilon(\omega)\boldsymbol{E}(\omega) \quad \text{and} \quad \boldsymbol{B}(\omega) = \mu_0\mu(\omega)\boldsymbol{H}(\omega), \tag{2.6}$$

where the symbols $\boldsymbol{D}, \boldsymbol{E}, \boldsymbol{B}$ and, $\boldsymbol{H}$ are reused to denote the electromagnetic fields as functions of the angular frequency ω. The permittivity, $\epsilon(\omega)$, and permeability, $\mu(\omega)$, are also functions of ω, with frequency dependencies restricted by the Kramers-Kronig relations [10, 13]. This relation follows from the analytic properties of $\epsilon(\omega)$ in $\operatorname{Im}\omega > 0$ (using time dependence $\mathrm{e}^{-\mathrm{i}\omega t}$) together with basic assumptions on the asymptotic properties of ϵ for low- and high frequencies. Here, an alternative approach is considered that is based on the additional assumption of passivity (2.3) and (2.4). This restricts ϵ such that $h_\epsilon = \omega\epsilon(\omega)$ is a Herglotz function [13, 21], *i.e.*, $h_\epsilon(\omega)$ is holomorphic and $\operatorname{Im} h_\epsilon(\omega) \geq 0$ in the upper halfplane $\operatorname{Im}\omega > 0$. The time-domain origin (2.1) imply the symmetry $h_\epsilon(\omega) = -h_\epsilon^*(-\omega^*)$, where a star denotes the complex conjugate. The permeability defines a similar Herglotz function $h_\mu(\omega) = \omega\mu(\omega)$. Note that the high-frequency asymptotic is consistent with the properties of Herglotz functions as a Herglotz function can not increase more than linearly for large ω, *i.e.*, $h(\omega) = \mathcal{O}(\omega)$ as $\omega\hat{\to}\infty$ [21], where the symbol $\hat{\to}$ is a short hand notation for limits in $\alpha < \arg\omega < \pi - \alpha$ for some $\alpha > 0$.

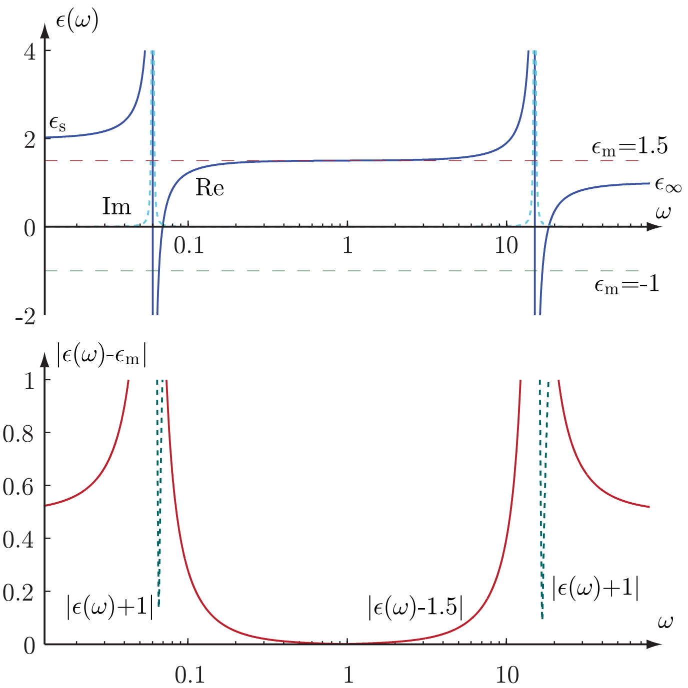

Figure 1: Illustration of the permittivity $\epsilon(\omega)$ in (2.8) with $\epsilon_{\rm s} = 2$ and $\epsilon_\infty = 1$ and the differences $|\epsilon(\omega) - \epsilon_{\rm m}|$ for $\epsilon_{\rm m} = 1.5$ and $\epsilon_{\rm m} = -1$. a) real-valued part (solid curves) and imaginary part (dashed curves). b) the differences $|\epsilon(\omega) - \epsilon_{\rm m}|$ for $\epsilon_{\rm m} = 1.5$ and $\epsilon_{\rm m} = -1$.

Herglotz functions can be represented as

$$h(z) = Az + \int_{\mathbb{R}} \left(\frac{1}{\xi - z} - \frac{\xi}{1+\xi^2} \right) \mathrm{d}\beta(\xi) = Az + \int_{\mathbb{R}} \frac{z}{\xi^2 - z^2} \,\mathrm{d}\beta(\xi), \tag{2.7}$$

where $\int (1+\xi^2)^{-1} \,\mathrm{d}\beta(\xi) < \infty$, $z = x + \mathrm{i}y$, $y > 0$, the symmetry is used in the second equality, and $\lim_{y\to 0} \operatorname{Im} h(\xi + \mathrm{i}y) \,\mathrm{d}\xi = \pi \,\mathrm{d}\beta(\xi)$ if $\operatorname{Im} h(\xi)$ is regular [11], *cf.*, the Kramers-Kronig relations [13].

2.2 A classical bound for lossless media

In this paper, we analyze how the basic assumptions (2.1) to (2.4) constrain the frequency dependence of the constitutive parameters. To start, consider a permittivity $\epsilon(\omega)$ with the low- and high-frequency asymptotes $\epsilon(0) = \epsilon_{\rm s}$ and $\epsilon(\infty) = \epsilon_\infty$, respectively. Simple examples show that the variation around $\epsilon_{\rm m} \in [\epsilon_\infty, \epsilon_{\rm s}]$ is not restricted by passivity, *e.g.*, the two-term Lorentz model

$$\epsilon(\omega) = \epsilon_\infty + \frac{\epsilon_{\rm s} - \epsilon_{\rm m}}{1 - (\omega/\omega_1)^2 - \mathrm{i}\nu\omega/\omega_1} + \frac{\epsilon_{\rm m} - \epsilon_\infty}{1 - (\omega/\omega_2)^2 - \mathrm{i}\nu\omega/\omega_2} \tag{2.8}$$

with $\omega_1 \ll \omega_0 \ll \omega_2$ and $\nu \ll 1$ has $\epsilon(\omega) \approx \epsilon_{\rm m}$ for a large bandwidth, see Fig. 1.

The example shows that the temporal dispersion does not restrict the frequency dependence for values $\epsilon_{\mathrm{m}} \in [\epsilon_\infty, \epsilon_{\mathrm{s}}]$. However, the example also shows that the temporal dispersion severely limits the bandwidth for $\epsilon(\omega) \approx \epsilon_{\mathrm{m}} = -1$. This is in general true and basic restrictions on the dispersion for lossless models of $\epsilon(\omega)$ and $\mu(\omega)$ can be obtained from the Kramers-Kronig relations [10, 13, 16] (Hilbert transform) or here by the representation (2.7). Consider an interval $[\omega_1, \omega_2]$ with $\mathrm{d}\beta(\xi) = 0$ (or equivalently $\operatorname{Im}\epsilon = 0$), then differentiation of $h(\omega)$ gives

$$\frac{\partial h_\epsilon}{\partial \omega}(\omega_0) = \epsilon_\infty + \int_{\mathbb{R}} \frac{1}{(\xi-\omega_0)^2}\,\mathrm{d}\beta(\xi) \geq \epsilon_\infty \tag{2.9}$$

for $\omega_1 < \omega_0 < \omega_2$. With $h_\epsilon(\omega) = \omega\epsilon(\omega)$, it shows that

$$\omega_0 \frac{\partial \epsilon}{\partial \omega}(\omega_0) \geq \epsilon_\infty - \epsilon(\omega_0). \tag{2.10}$$

The derivative of $\epsilon(\omega_0)$ is hence positive in intervals where $\operatorname{Im}\epsilon(\omega) = 0$ and $\epsilon(\omega_0) < \epsilon_\infty$. A sharper bound follows from [16]

$$\frac{\partial \omega h_\epsilon}{\partial \omega}(\omega_0) = 2\omega_0\epsilon_\infty + \int_{\mathbb{R}} \frac{\xi}{(\xi-\omega_0)^2}\,\mathrm{d}\beta(\xi) \geq 2\omega_0\epsilon_\infty \tag{2.11}$$

for $\omega_1 < \omega_0 < \omega_2$. With $h_\epsilon(\omega) = \omega\epsilon(\omega)$, it shows that

$$\omega_0 \frac{\partial \epsilon}{\partial \omega}(\omega_0) \geq 2(\epsilon_\infty - \epsilon(\omega_0)). \tag{2.12}$$

In particular, the restrictions on $\frac{\partial\epsilon}{\partial\omega}$ increases as $\epsilon(\omega_0)$ decreases. The constraint (2.12) is transformed into a bound on the variation around ϵ_{m} over a fractional bandwidth $B = (\omega_2 - \omega_1)/\omega_0$ around the center frequency $\omega_0 = (\omega_2 + \omega_1)/2$ by observing that $\frac{\partial\epsilon(\omega)}{\partial\omega} \geq \frac{\partial\epsilon(\omega_0)}{\partial\omega}$ for $\omega_1 < \omega \leq \omega_0$ and hence, with $\epsilon(\omega_0) = \epsilon_{\mathrm{m}}$

$$\epsilon_{\mathrm{m}} - \epsilon(\omega_1) = \int_{\omega_1}^{\omega_0} \frac{\partial \epsilon(\omega)}{\partial \omega}\,\mathrm{d}\omega \geq 2\frac{\omega_1 - \omega_0}{\omega_0}(\epsilon_\infty - \epsilon_{\mathrm{m}}). \tag{2.13}$$

This can be rewritten as

$$\max_{\omega\in\mathcal{B}} |\epsilon(\omega) - \epsilon_{\mathrm{m}}| \geq B(\epsilon_\infty - \epsilon_{\mathrm{m}}) \tag{2.14}$$

which demonstrates that the deviation of $\epsilon(\omega)$ around ϵ_{m} is proportional to the fractional bandwidth, B, in the interval $\mathcal{B} = [\omega_1, \omega_2]$ where the material model is lossless.

The pointwise bound on the derivative (2.12) is not true when losses are present, even if the loss (*i.e.*, the imaginary part $\operatorname{Im} h(\omega)$) is arbitrarily small. Consider, *e.g.*, the Lorentz model

$$h_\epsilon(\omega) = \epsilon_\infty\omega + \frac{\omega\nu^{3/2}}{1-\omega^2-\mathrm{i}\nu\omega}, \tag{2.15}$$

where $\epsilon_\infty > 0$ and $\nu \geq 0$. It has $h(1) = \epsilon_\infty + \mathrm{i}\nu^{1/2} \approx \epsilon_\infty$ for $\nu \ll 1$ but

$$\frac{\partial h_\epsilon}{\partial \omega}(1) = \epsilon_\infty + \mathrm{i}\nu^{1/2} - \frac{2+\mathrm{i}\nu}{\nu^{1/2}} = \epsilon_\infty - \frac{2}{\nu^{1/2}} \to -\infty \quad \text{as } \nu \to 0. \tag{2.16}$$

This simple example shows that it is very difficult to bound the derivative of Herglotz functions (and hence ϵ and μ) pointwise. The requirements of lossless material models are removed in [17], where it is shown that $|\epsilon(\omega)+1| \geq B$ for all square integrable susceptibilities $\epsilon(\omega)-1$.

2.3 Construction of sum rules

Here, it is shown that bounds similar to (2.14) are valid for all passive constitutive relations of the form (2.6). It is also shown that the difference $\epsilon_{\rm s}-\epsilon_\infty$ further restricts the bandwidth. The results are based on sum rules obtained by considering weighted integrals applied to Herglotz functions under the assumption of the following asymptotic expansions at low frequencies: $h(\omega)=\sum_n a_{2n-1}\omega^{2n-1}+\mathrm{o}(\omega^{2N_0-1})$ as $k\hat{\to}0$, and at high frequencies, $h(\omega)=\sum_n b_{2n-1}\omega^{1-2n}+\mathrm{o}(\omega^{-2N_\infty+1})$ as $k\hat{\to}\infty$. The results are restricted to Herglotz functions satisfying the cross symmetry $h(\omega)=-h^*(-\omega^*)$, where a star denotes the complex conjugate, and hence to real valued a_n and b_n for odd n, giving the following family of integral identities:

$$\frac{2}{\pi}\int_0^\infty \frac{\operatorname{Im} h(\omega)}{\omega^{2n}}\,\mathrm{d}\omega = a_{2n-1}-b_{1-2n}, \tag{2.17}$$

for $1-N_\infty \leq n \leq N_0$. Physical bounds are obtained by bounding the integral from below by restricting it to a finite interval [3–6, 8, 9, 23, 30, 31].

The sum rules generated by h_ϵ and h_μ with no static conductivity are identical to the ones obtained from the Kramers-Kronig relations [10, 13, 16], *e.g.*,

$$\frac{2}{\pi}\int_0^\infty \frac{\operatorname{Im} h_\epsilon(\omega)}{\omega^2}\,\mathrm{d}\omega = \frac{2}{\pi}\int_0^\infty \frac{\operatorname{Im} \epsilon(\omega)}{\omega}\,\mathrm{d}\omega = \epsilon_{\rm s}-\epsilon_\infty. \tag{2.18}$$

This sum rule relates the losses to the asymptotic values and it shows that $\epsilon_{\rm s} \geq \epsilon_\infty$. Compositions of Herglotz functions are used to create new Herglotz functions that instead relate the variation around a fixed value, *e.g.*, $\epsilon_{\rm m}$, to the corresponding asymptotes.

As the Herglotz identities (2.17) relate the imaginary part of the function with its asymptotic values, it is necessary to transform the Herglotz function such that the imaginary part is of primary interest. Construct a Herglotz function, $h_\varDelta(z)$, with an imaginary part given by $\operatorname{Im} h_\varDelta(x)=1$ for $|x|<\varDelta$ and $\operatorname{Im} h_\varDelta(x)=0$ for $|x|>\varDelta$, where $z=x+\mathrm{i}y$ with $y>0$. Analytic continuation using the representation (2.7) gives

$$h_\varDelta(z)=\frac{1}{\pi}\int_{-\varDelta}^{\varDelta}\frac{1}{\xi-z}\,\mathrm{d}\xi=\frac{1}{\pi}\ln\frac{z-\varDelta}{z+\varDelta}, \quad \text{for } \operatorname{Im} z>0 \tag{2.19}$$

Here, the logarithm has its branch cut along the negative real axis. The imaginary part is bounded by unity and the region with $1 \geq \operatorname{Im} h_\varDelta(z) \geq \zeta \geq 1/2$ is given by the union of the circle

$$x^2+\left(y-\frac{\varDelta}{\tan(\pi\zeta)}\right)^2 \leq \varDelta^2\left(1+\frac{1}{\tan^2(\pi\zeta)}\right) \tag{2.20}$$

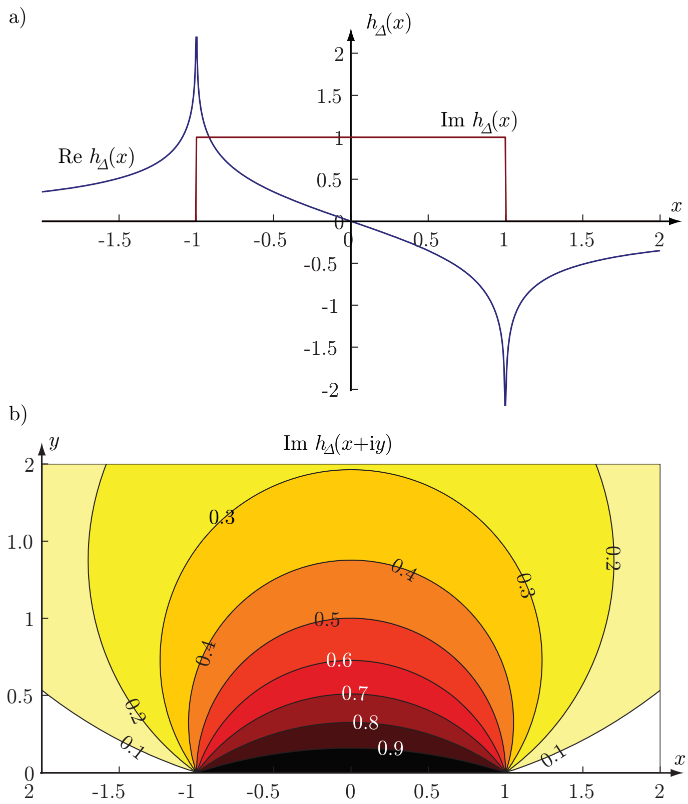

Figure 2: Illustrations of the Herglotz function $h_\Delta(z)$ in (2.19) with $\Delta = 1$. a) real and imaginary parts for $\operatorname{Im} z = 0$. b) contour plot of $\operatorname{Im} h_\Delta(x + \mathrm{i}y)$.

and the plane $y > 0$, see Fig. 2. Note that the circle intersects the points $z = \pm\Delta$ and $z = \mathrm{i}\Delta 2\sin^2(\pi\zeta/2)/\sin(\pi\zeta)$ and in particular $\operatorname{Im} h_\Delta(z) \geq 1/2$ for $|z| \leq \Delta$. The asymptotes of (2.19) are

$$h_\Delta(z) \sim \begin{cases} 1, & \text{as } z\hat{\to}0 \\ \frac{-2\Delta}{\pi z}, & \text{as } z\hat{\to}\infty \end{cases} \tag{2.21}$$

where $\sim$ denotes asymptotic similar, defined as $h(\omega) \sim h_1(\omega)$ as $\omega\hat{\to}\infty$ if $h(\omega) = h_1(\omega) + \mathrm{o}(|h_1(\omega)|)$ as $\omega\hat{\to}\infty$. The function (2.19) is useful to restrict the interval where the amplitude of a Herglotz function is small, as compositions of h_Δ with *e.g.*, h_ϵ maps regions where $|h_\epsilon| < \Delta$ to imaginary values between 1/2 and 1.

3 Sum rules for metamaterials

In this section, four sum rules are used to derive bounds for different a priori knowledge of the low- and high-frequency asymptotes. In Sec. 3.1 sum rules independent of the low-frequency asymptote are derived which gives a bound expressed in the difference between the target value and the high-frequency asymptote. Sum rules valid for models without a static conductivity are derived in Sec. 3.2 which produces a bound proportional to the difference between the high- and low-frequency asymptotes. The third sum rule in Sec. 3.3 constrains parameter values larger than the static limit and is particular interesting for artificial magnets. The final sum rules derived in Sec. 3.4 are identities expressed in the plasma frequency.

3.1 Bounds expressed in the instantaneous response

Consider a permittivity $\epsilon(\omega)$ with the high-frequency asymptotes ϵ_∞ obtained from (2.1) and construct the Herglotz function

$$h_1(\omega) = \frac{\omega}{\omega_0}\big(\epsilon(\omega) - \epsilon_{\mathrm{m}}\big) \sim \begin{cases} \mathcal{O}(1), & \text{as } z\hat{\to}0 \\ \frac{\omega(\epsilon_\infty - \epsilon_{\mathrm{m}})}{\omega_0}, & \text{as } z\hat{\to}\infty \end{cases} \tag{3.1}$$

where $\epsilon_{\mathrm{m}} < \epsilon_\infty$ is the desired value of $\epsilon(\omega)$ around $\omega = \omega_0$. It has the property $h_1(\omega) \approx 0$ if $\epsilon(\omega) \approx \epsilon_{\mathrm{m}}$. Compose h_Δ with h_1 to construct a new Herglotz function, *i.e.*,

$$h_{\Delta 1}(\omega) = h_\Delta(h_1(\omega)) \sim \begin{cases} \mathcal{O}(1), & \text{as } z \to 0 \\ \frac{-2\omega_0\Delta}{\omega\pi(\epsilon_\infty - \epsilon_{\mathrm{m}})}, & \text{as } z \to \infty \end{cases} \tag{3.2}$$

These asymptotes show that $h_{\Delta 1}$ has an $n = 0$ sum rule in (2.17), *i.e.*,

$$\int_0^\infty \mathrm{Im}\, h_{\Delta 1}(\omega)\,\mathrm{d}\omega = \int_0^\infty \frac{1}{\pi} \arg\Big(\frac{\omega\big(\epsilon(\omega) - \epsilon_{\mathrm{m}}\big) - \omega_0\Delta}{\omega\big(\epsilon(\omega) - \epsilon_{\mathrm{m}}\big) + \omega_0\Delta}\Big)\,\mathrm{d}\omega = \frac{\omega_0\Delta}{\epsilon_\infty - \epsilon_{\mathrm{m}}}. \tag{3.3}$$

The properties of this sum rule are easiest to understand for intervals with $\mathrm{Im}\,\epsilon(\omega) \approx 0$, where it is seen that the integrand is approximately one or zero depending on whether $|h_1(\omega)|$ is smaller or larger than Δ, respectively. This is made more precise by consideration of a function $h_1(\omega)$ that is restricted to the region defined by ζ in (2.20) over the interval $\omega \in \mathcal{B} = [\omega_1, \omega_2]$ with $\omega_0 = (\omega_2 + \omega_1)/2$ and $B = (\omega_2 - \omega_1)/\omega_0$. The integral (3.3) is then bounded as

$$B \min_{\omega\in\mathcal{B}} \mathrm{Im}\, h_\Delta(h_1(\omega)) \leq \frac{1}{\omega_0}\int_{\omega_1}^{\omega_2} \mathrm{Im}\, h_{\Delta 1}(\omega)\,\mathrm{d}\omega \leq \frac{\Delta}{\epsilon_\infty - \epsilon_{\mathrm{m}}} \tag{3.4}$$

and in particular in lossy and lossless cases

$$\min_{\omega\in\mathcal{B}} \mathrm{Im}\, h_\Delta(h_1(\omega)) \geq \begin{cases} 1/2 & \text{for } \max_{\omega\in\mathcal{B}} |h_1(\omega)| = \Delta \\ 1 & \text{for } \max_{\omega\in\mathcal{B}} |h_1(\omega)| = \Delta \text{ and } \max_{\omega\in\mathcal{B}} |\mathrm{Im}\, h_1(\omega)| = 0 \end{cases} \tag{3.5}$$

giving

$$\max_{\omega\in\mathcal{B}} |h_1(\omega)| \geq B(\epsilon_\infty - \epsilon_{\mathrm{m}}) \begin{cases} 1/2 & \text{lossy case} \\ 1 & \text{lossless case,} \end{cases} \tag{3.6}$$

The bound (3.6) on $h_1 = \omega(\epsilon - \epsilon_{\mathrm{m}})/\omega_0$ is transformed into a bound on $\epsilon - \epsilon_{\mathrm{m}}$ as

$$\max_{\omega\in\mathcal{B}} |\epsilon(\omega) - \epsilon_{\mathrm{m}}| \geq \frac{B}{1 + B/2}(\epsilon_\infty - \epsilon_{\mathrm{m}}) \begin{cases} 1/2 & \text{lossy case} \\ 1 & \text{lossless case,} \end{cases} \tag{3.7}$$

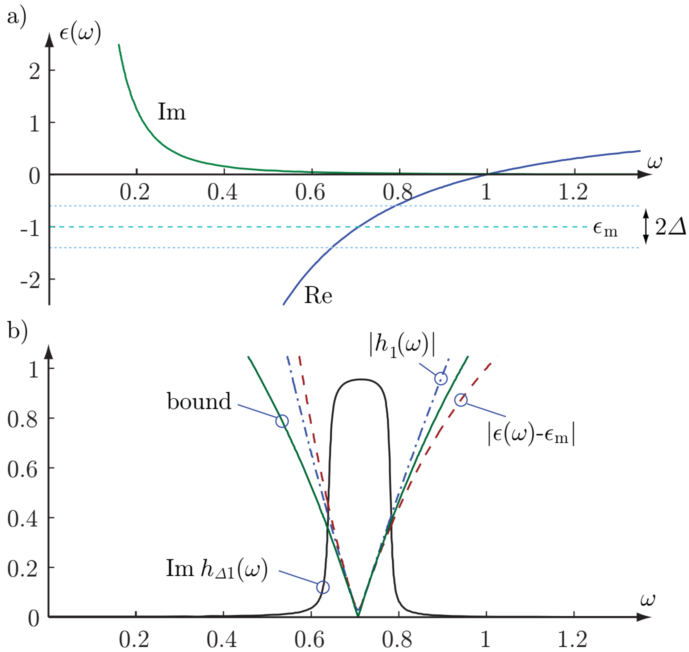

Figure 3: Illustrations of the Drude model (3.8) with the sum rule (3.3) and bound (3.7). a) the permittivity $\epsilon(\omega)$. b) the integrand in the sum rule (3.3), $\operatorname{Im} h_{\Delta 1} = \operatorname{Im} h_{\Delta}(h_1)$, the function $|h_1|$, the difference $|\epsilon - \epsilon_{\rm m}|$, and the bandwidth bound (3.4) with $\epsilon_{\rm m} = -1$ and $\Delta = 0.4$.

where the bound in lossy media is identical to the bound in [17] for $B \ll 1$, $\epsilon_\infty = 1$, and $\epsilon_{\rm m} = -1$.

As an example consider the Drude model

$$\epsilon(\omega) = 1 + \frac{1}{-\mathrm{i}\omega(0.01 - \mathrm{i}\omega)}, \tag{3.8}$$

where ω is a dimensionless frequency variable and the plasma frequency is $\omega_{\rm p} = 1$, see Fig. 3a. It has a negative real part for $\omega < 1$. The sum rule (3.3) is evaluated for $\epsilon_{\rm m} = -1$ and $\Delta = 0.4$. The integrand in (3.3) is depicted in Fig. 3b, where it is observed that it has most of its area in the region around $\omega_0 \approx 0.7$, *i.e.*, in the region where $|\epsilon(\omega) - \epsilon_{\rm m}| \approx \operatorname{Re}\epsilon(\omega) - \epsilon_{\rm m} \leq \Delta$. The amplitudes $|h_1(\omega)|$ and $|\epsilon(\omega) - \epsilon_{\rm m}|$ together with the bandwidth bound (3.4) are also included in the figure. The bound states that $\epsilon(\omega)$ can not be designed such that its bandwidth is wider than the bound depicted in Fig. 3b.

The sum rule (3.3) and bounds (3.7) are valid with or without a static conductivity. The corresponding results for the permeability μ are obtained by substitution of μ for ϵ in (3.1) to (3.7). They are also valid for the refractive index $n(\omega)$ defined by the square-root composition of $\omega\epsilon$ and $\omega\mu$, *i.e.*, the Herglotz function $h_{\rm n} = \omega n = \mathrm{i}\sqrt{-h_\epsilon h_\mu} = \mathrm{i}\sqrt{-\omega^2\epsilon\mu}$. Here, the square root has its branch cut along the negative real axis and the minus sign inside the square root and multiplication with the imaginary unit are essential steps to preserve the symmetry and the Her-

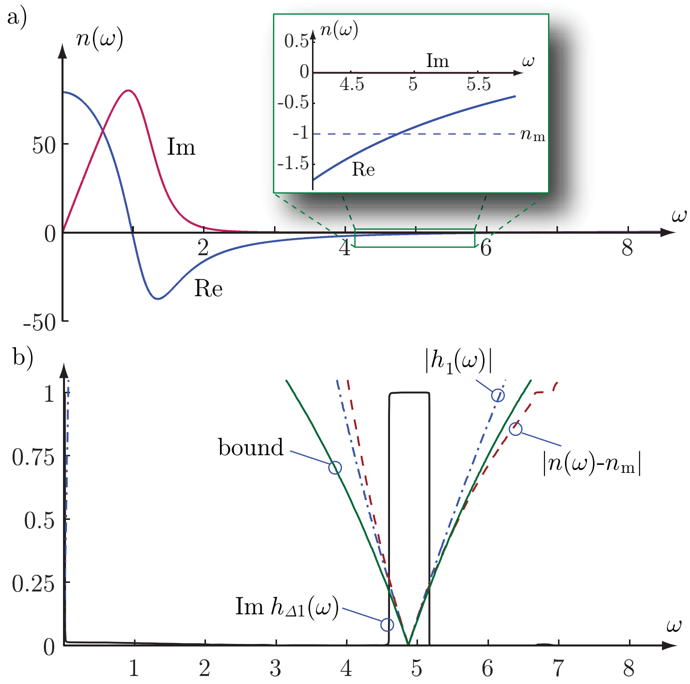

Figure 4: Illustrations of the model (3.9) with $n_{\mathrm{m}} = -1$. a) the refractive index $n(\omega)$. b) integrand (solid curved) of the sum rule (3.3), $|h_1(\omega)|$, $|n(\omega) - n_{\mathrm{m}}|$, and bandwidth bound (3.7).

glotz property. Let n_∞ denote the instantaneous response of the refractive index, *i.e.*, $n(\omega) \sim n_\infty$ as $\omega\hat{\to}\infty$. It is often assumed that $n_\infty \geq 1$ to ensure consistency with the upper bound set by the speed of light in free space [10, 16]. The corresponding instantaneous permittivity, $\epsilon_\infty > 0$, and permeability, $\mu_\infty > 0$, are related through $\epsilon_\infty\mu_\infty = n_\infty^2$.

A numerical example with negative index of refraction and low losses over a broad frequency range is suggested in [18]. It is generated by the Kramers-Kronig relations [10, 13] using the imaginary parts

$$\operatorname{Im}\epsilon(\omega) = 0.9\frac{\omega(\omega^2-25)^2}{\omega^8+5.5}, \quad \text{and} \quad \operatorname{Im}\mu(\omega) = 0.7\frac{\omega(\omega^2-25)^2}{\omega^8+4.2}. \tag{3.9}$$

The index of refraction $n = \mathrm{i}\sqrt{-\epsilon\mu}$ is depicted in 4a and it has $n(0) \approx 79$, $n_\infty = 1$, $\omega_{\mathrm{p}} \approx 6.7$, and $n(\omega_0) \approx -1$, where $\omega_0 \approx 4.9$. The integrand in the sum rules (3.3) for $n(\omega) \approx -1$ and $\mathit{\Delta} = 0.25$ is depicted in Fig. 4. It is observed that the area is concentrated around ω_0.

3.2 Metamaterials without a static conductivity

The low-frequency asymptotes of ϵ, μ, and n depend on the presence of static conductivity. In the case with no static conductivity, the linear response of $h_\epsilon(\omega) =$

$\epsilon_{\mathrm{s}}\omega + \mathrm{o}(\omega)$ as $\omega\hat{\to}0$ results in sum rules expressed in the static permittivity ϵ_{s}. Consider a permittivity with high-frequency limit $\epsilon_\infty \geq 0$ and a desired permittivity $\epsilon_{\mathrm{m}} \leq \epsilon_\infty$. The corresponding results for the permeability and index of refraction are obtained from the corresponding permittivity sum rules with the substitution of μ or n for ϵ.

A sum rule that incorporates the static permittivity ϵ_{s} in the bound on $|\epsilon(\omega)-\epsilon_{\mathrm{m}}|$ is constructed from the Herglotz function

$$h_2(\omega) = -\frac{\omega_0}{\omega}\frac{\epsilon_\infty-\epsilon_{\mathrm{m}}}{\epsilon(\omega)-\epsilon_\infty} - \frac{\omega_0}{\omega} = -\frac{\omega_0}{\omega}\frac{\epsilon(\omega)-\epsilon_{\mathrm{m}}}{\epsilon(\omega)-\epsilon_\infty} \sim \begin{cases} \frac{-\omega_0}{\omega}\frac{\epsilon_{\mathrm{s}}-\epsilon_{\mathrm{m}}}{\epsilon_{\mathrm{s}}-\epsilon_\infty} & \text{as } \omega\hat{\to}0 \\ \mathcal{O}(\omega) & \text{as } \omega\hat{\to}\infty \end{cases} \tag{3.10}$$

that has the property $|h_2(\omega)| \approx 0$ if $\epsilon(\omega) \approx \epsilon_{\mathrm{m}}$. Compose (3.10) with (2.19) to get the Herglotz function

$$h_{\Delta 2}(\omega) = h_\Delta(h_2(\omega)) \sim \begin{cases} \frac{2\omega\Delta}{\omega_0\pi}\frac{\epsilon_{\mathrm{s}}-\epsilon_\infty}{\epsilon_{\mathrm{s}}-\epsilon_{\mathrm{m}}}, & \text{as } \omega\hat{\to}0 \\ \mathrm{o}(\omega), & \text{as } \omega\hat{\to}\infty \end{cases} \tag{3.11}$$

It has the $n=1$ sum rule

$$\int_0^\infty \frac{\omega_0^2}{\omega^2\pi}\arg\left(\frac{\omega_0\big(\epsilon(\omega)-\epsilon_{\mathrm{m}}\big)+\omega\Delta\big(\epsilon(\omega)-\epsilon_\infty\big)}{\omega_0\big(\epsilon(\omega)-\epsilon_{\mathrm{m}}\big)-\omega\Delta\big(\epsilon(\omega)-\epsilon_\infty\big)}\right)\mathrm{d}\omega = \omega_0\Delta\frac{\epsilon_{\mathrm{s}}-\epsilon_\infty}{\epsilon_{\mathrm{s}}-\epsilon_{\mathrm{m}}} \tag{3.12}$$

Bound the integral as in (3.4) to get

$$B\min_{\omega\in\mathcal{B}}\operatorname{Im} h_\Delta(h_2(\omega)) \leq \Delta\frac{\epsilon_{\mathrm{s}}-\epsilon_\infty}{\epsilon_{\mathrm{s}}-\epsilon_{\mathrm{m}}} \tag{3.13}$$

and finally

$$\max_{\omega\in\mathcal{B}}\frac{|\epsilon(\omega)-\epsilon_{\mathrm{m}}|}{|\epsilon(\omega)-\epsilon_\infty|} \geq \frac{B}{1+B/2}\frac{\epsilon_{\mathrm{s}}-\epsilon_{\mathrm{m}}}{\epsilon_{\mathrm{s}}-\epsilon_\infty}\begin{cases} 1/2 & \text{lossy case} \\ 1 & \text{lossless case} \end{cases} \tag{3.14}$$

The sum rule (3.12) and bound (3.14) show that the constraints on the variation of ϵ around ϵ_{m} is proportional to the difference $\epsilon_{\mathrm{s}}-\epsilon_\infty$. It is hence necessary to have a static permittivity $\epsilon_{\mathrm{s}} > 1$ or a small instantaneous response $\epsilon_\infty < 1$ for broadband performance. Note that these results are valid for the case $\epsilon_\infty = 0$, although it is in general very difficult to show that the time-domain Maxwell equations are well posed in this case.

As an example, the classical Lorentz model is considered for the permittivity

$$\epsilon(\omega) = 1 + \frac{0.2}{1-\omega^2-0.001\mathrm{i}\omega} \tag{3.15}$$

that has $\epsilon_\infty = 1$ and $\epsilon_{\mathrm{s}} = 1.2$. It is not a particularly good candidate for $\epsilon_{\mathrm{m}} = -1$ materials but is has a narrow frequency range around $\omega = 1.05\omega_0$ where $\operatorname{Re}\epsilon \approx -1$. The integrand of the sum rules (3.10) is depicted in Fig. 5. for $\epsilon_{\mathrm{m}} = -1$ and $\Delta = 0.2$.

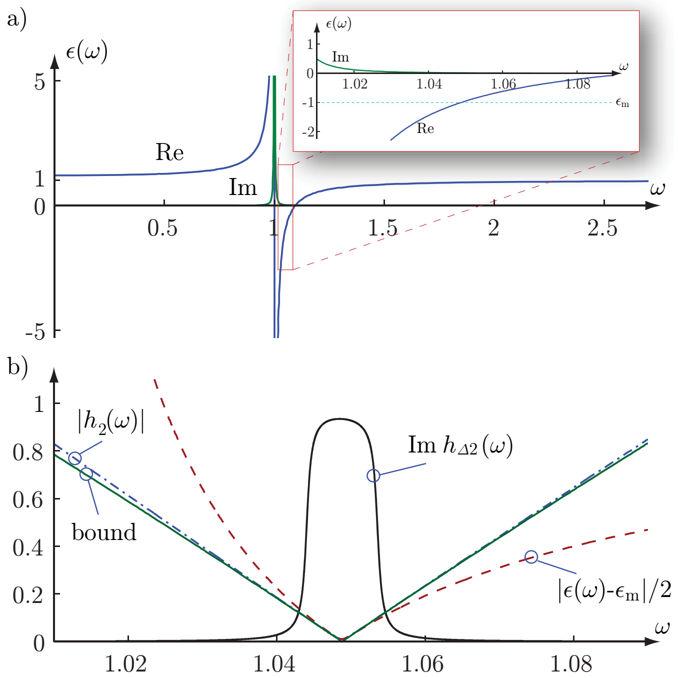

Figure 5: Illustrations of a Lorentz model (3.15) and sum rules. a) the permittivity $\epsilon(\omega)$. b) imaginary part of the integrand of the sum rule (3.12).

Although an effective small-signal magnetic conductivity can theoretically be created in suitably biased ferromagnetic material [22], we exclude the possibility of a static magnetic conductivity in linear, passive materials as considered in this paper. Thus, the corresponding sum rules and bounds for permeability are given by simply replacing ϵ by μ in the preceding equations.

If a static electric conductivity is present, the low-frequency asymptote of n is $h_{\rm n}(\omega) = \mathcal{O}(\omega^{1/2})$ as $\omega \hat{\to} 0$. The sum rules and bounds for the refractive index are then given by replacing ϵ by n and replacing the static value by infinity, $n_{\rm s} = \infty$. It is seen that in the sum rules and bounds, the right hand side is maximized if the static material properties are large. This implies that the bounds are generally tighter for permeability than for permittivity and refractive index if an electrical conductivity is present.

3.3 Artificial permeability

In applications with artificial magnetics, it is desired to design materials with a permeability, $\mathrm{Re}\,\mu(\omega)$ larger than its static value $\mu_{\rm s}$, *i.e.*, $\mu(\omega_0) \approx \mu_{\rm m} > \mu_{\rm s}$. Consider the Herglotz function

$$h_3(\omega) = -\frac{\omega_0(\mu_{\rm m} - \mu_\infty)}{\omega(\mu(\omega) - \mu_\infty)} + \frac{\omega_0}{\omega} = \frac{\omega_0}{\omega}\frac{\mu(\omega) - \mu_{\rm m}}{\mu(\omega) - \mu_\infty} \sim \begin{cases} -\frac{\omega_0}{\omega}\frac{\mu_{\rm m}-\mu_{\rm s}}{\mu_{\rm s}-\mu_\infty} & \text{as } \omega \hat{\to} 0 \\ \mathcal{O}(\omega) & \text{as } \omega \hat{\to} \infty \end{cases} \tag{3.16}$$

where $\mu_{\rm m} > \mu_{\rm s}$. Compose with h_Δ to get the Herglotz function $h_{\Delta 3}$ with the asymptotes

$$h_{\Delta 3}(\omega) = h_\Delta(h_3(\omega)) \sim \begin{cases} \frac{2\omega\Delta}{\pi\omega_0}\frac{\mu_{\rm s}-\mu_\infty}{\mu_{\rm m}-\mu_{\rm s}} & \text{as } \omega\hat{\to}0 \\ \mathcal{O}(\omega^{-1}) & \text{as } \omega\hat{\to}\infty \end{cases} \tag{3.17}$$

and the sum rule

$$\int_0^\infty \frac{\omega_0^2}{\omega^2\pi}\arg\Big(\frac{h_3(\omega)+\Delta}{h_3(\omega)-\Delta}\Big)\,{\rm d}\omega = \omega_0\Delta\frac{\mu_{\rm s}-\mu_\infty}{\mu_{\rm m}-\mu_{\rm s}} \tag{3.18}$$

with the bound

$$\max_{\omega\in\mathcal{B}}\frac{|\mu(\omega)-\mu_{\rm m}|}{|\mu(\omega)-\mu_\infty|} \geq \frac{B}{1+B/2}\frac{\mu_{\rm m}-\mu_{\rm s}}{\mu_{\rm s}-\mu_\infty}\begin{cases}1/2 & \text{lossy case}\\ 1 & \text{lossless case}\end{cases} \tag{3.19}$$

The Lorentz model is a common resonance model that has a narrow frequency range with values larger than its static value. Here, it used to illustrate the sum rule (3.18) and bound (3.19) on artificial permeability. Consider a permeability

$$\mu(\omega) = 1 + \frac{2}{1-\omega^2-0.01{\rm i}\omega} \tag{3.20}$$

that has $\mu_\infty = 1$ and $\mu_{\rm s} = 3$. It is has a narrow frequency range around $\omega = 0.9$ where ${\rm Re}\,\mu \approx \mu_{\rm m} = 10$. The integrand of the sum rules (3.18) is depicted in Fig. 5. for $\epsilon_{\rm m} = 10$ and $\Delta = 0.5$.

3.4 Bounds expressed in the plasma frequency

A priori information about the plasma frequency can be used to derive additional sum rules and constraints on metamaterials. It is often assumed that, *e.g.*, $\epsilon(\omega) \sim \epsilon_\infty - \omega_{\rm p}^2/\omega^2$ as $\omega \to \infty$, where $\omega_{\rm p}$ is the plasma frequency [10].

A sum rule involving the plasma frequency $\omega_{\rm p}$ is constructed from the Herglotz function h_2 in (3.10) with the high-frequency asymptote $h_2(\omega) \sim \frac{\omega\omega_0}{\omega_{\rm p}^2}(\epsilon_\infty - \epsilon_{\rm m})$ as $\omega\hat{\to}\infty$ and

$$h_\Delta(h_2(\omega)) \sim \begin{cases}\mathcal{O}(\omega) & \text{as } \omega\hat{\to}0\\ \frac{-2\omega_{\rm p}^2\Delta}{\pi\omega\omega_0(\epsilon_\infty-\epsilon_{\rm m})} & \text{as } \omega\hat{\to}\infty\end{cases} \tag{3.21}$$

It has an $n=0$ sum rule, *viz.*,

$$\int_0^\infty \frac{1}{\pi}\arg\Big(\frac{\omega_0\big(\epsilon(\omega)-\epsilon_{\rm m}\big)+\Delta\omega\big(\epsilon(\omega)-\epsilon_\infty\big)}{\omega_0\big(\epsilon(\omega)-\epsilon_{\rm m}\big)-\Delta\omega\big(\epsilon(\omega)-\epsilon_\infty\big)}\Big)\,{\rm d}\omega = \frac{\omega_{\rm p}^2\Delta}{\omega_0(\epsilon_\infty-\epsilon_{\rm m})} \tag{3.22}$$

and the associate physical bound

$$\max_{\omega\in\mathcal{B}}\frac{|\epsilon(\omega)-\epsilon_{\rm m}|}{|\epsilon(\omega)-\epsilon_\infty|} \geq \frac{B}{1+B/2}\frac{\omega_0^2}{\omega_{\rm p}^2}(\epsilon_\infty-\epsilon_{\rm m})\begin{cases}1/2 & \text{lossy case}\\ 1 & \text{lossless case}\end{cases} \tag{3.23}$$

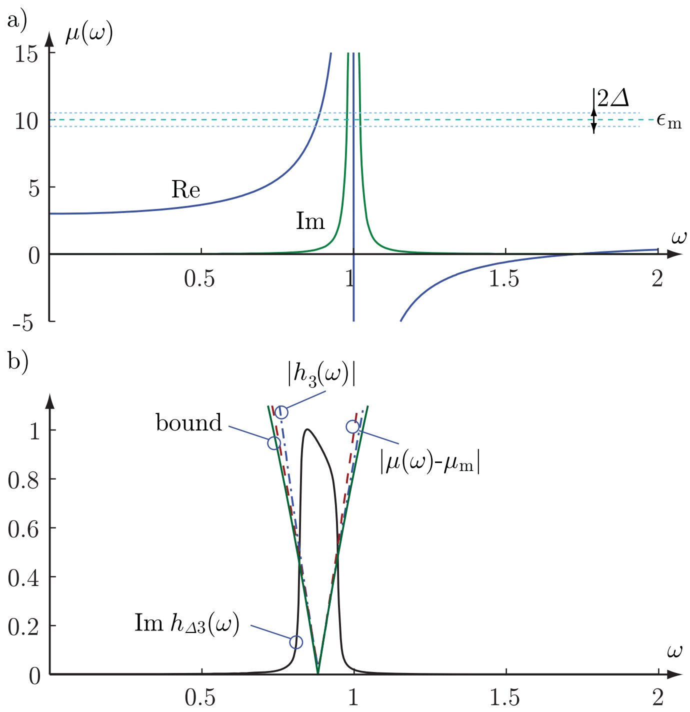

Figure 6: Illustrations of the Lorentz model (3.20) and sum rule (3.18) for artificial permeability. a) the permeability $\mu(\omega)$. b) imaginary part of the integrand of the sum rule (3.18).

The Herglotz function h_3 in (3.16) with $\mu(\omega) \sim \mu_\infty - \omega_{\mathrm{p}}^2/\omega^2$ as $\omega \hat{\to} \infty$ has the high-frequency asymptote $h_3(\omega) \sim (\mu_{\mathrm{m}} - \mu_\infty)\omega\omega_0/\omega_{\mathrm{p}}^2$ giving

$$h_\Delta(h_3(\omega)) \sim \begin{cases} \mathcal{O}(\omega) & \text{as } \omega \hat{\to} 0 \\ \frac{-2\omega_{\mathrm{p}}^2 \Delta}{\pi\omega\omega_0(\mu_{\mathrm{m}} - \mu_\infty)} & \text{as } \omega \hat{\to} \infty \end{cases} \tag{3.24}$$

for $\mu_{\mathrm{m}} > \mu_{\mathrm{s}}$ giving the sum rule

$$\int_0^\infty \frac{1}{\pi} \arg\left(\frac{h_3(\omega) + \Delta}{h_3(\omega) - \Delta}\right) \mathrm{d}\omega = \frac{\omega_{\mathrm{p}}^2 \Delta}{\omega_0(\mu_{\mathrm{m}} - \mu_\infty)} \tag{3.25}$$

with the bound

$$\max_{\omega \in \mathcal{B}} \frac{|\mu(\omega) - \mu_{\mathrm{m}}|}{|\mu(\omega) - \mu_\infty|} \geq \frac{B}{1 + B/2} \frac{\omega_0^2}{\omega_{\mathrm{p}}^2} (\mu_{\mathrm{m}} - \mu_\infty) \begin{cases} 1/2 & \text{lossy case} \\ 1 & \text{lossless case} \end{cases} \tag{3.26}$$

The bounds show that it is advantageous to have $\omega_0 < \omega_{\mathrm{p}}$ for good performance.

4 Bi-anisotropic constitutive relations

The constitutive relations treated in this paper can be augmented to include so called bi-anisotropic materials. These are materials where the relation between the

$[\boldsymbol{E},\boldsymbol{H}]$ and $[\boldsymbol{D},\boldsymbol{B}]$ fields is written in the frequency domain as

$$\begin{pmatrix}\boldsymbol{D}(\omega)\\ \boldsymbol{B}(\omega)\end{pmatrix} = \begin{pmatrix}\epsilon_0\boldsymbol{\epsilon}(\omega) & \mathrm{c}_0^{-1}\boldsymbol{\xi}(\omega)\\ \mathrm{c}_0^{-1}\boldsymbol{\zeta}(\omega) & \mu_0\boldsymbol{\mu}(\omega)\end{pmatrix}\begin{pmatrix}\boldsymbol{E}(\omega)\\ \boldsymbol{H}(\omega)\end{pmatrix} \tag{4.1}$$

where the dimensionless $\boldsymbol{\epsilon}$, $\boldsymbol{\xi}$, $\boldsymbol{\zeta}$, and $\boldsymbol{\mu}$ are now matrix-valued functions of ω. The material is passive if the total dissipated power is non-negative [12], *i.e.*, the imaginary part of all hermitian quadratic forms over the 6×6 material matrix weighted by ω are non-negative,

$$\mathrm{Im}\left\{\omega\begin{pmatrix}\boldsymbol{E}(\omega)^*\\ \boldsymbol{H}(\omega)^*\end{pmatrix}\cdot\begin{pmatrix}\epsilon_0\boldsymbol{\epsilon}(\omega) & \mathrm{c}_0^{-1}\boldsymbol{\xi}(\omega)\\ \mathrm{c}_0^{-1}\boldsymbol{\zeta}(\omega) & \mu_0\boldsymbol{\mu}(\omega)\end{pmatrix}\begin{pmatrix}\boldsymbol{E}(\omega)\\ \boldsymbol{H}(\omega)\end{pmatrix}\right\}\geq 0 \quad \text{for all } \boldsymbol{E} \text{ and } \boldsymbol{H} \tag{4.2}$$

Choosing $[\boldsymbol{E}(\omega),\boldsymbol{H}(\omega)] = E_0[\boldsymbol{e}_0,\eta_0^{-1}\boldsymbol{h}_0]$ where E_0 is a normalization constant and $\boldsymbol{e}_0$ and $\boldsymbol{h}_0$ are dimensionless, constant and real-valued vectors, the dimensionless quadratic form

$$q(\omega) = \begin{pmatrix}\boldsymbol{e}_0\\ \boldsymbol{h}_0\end{pmatrix}\cdot\begin{pmatrix}\boldsymbol{\epsilon}(\omega) & \boldsymbol{\xi}(\omega)\\ \boldsymbol{\zeta}(\omega) & \boldsymbol{\mu}(\omega)\end{pmatrix}\begin{pmatrix}\boldsymbol{e}_0\\ \boldsymbol{h}_0\end{pmatrix} \tag{4.3}$$

then defines a Herglotz function $h_q(\omega) = \omega q(\omega)$ for each fixed vector pair $[\boldsymbol{e}_0,\boldsymbol{h}_0]$, and all the previous sum rules apply to $q(\omega)$. The vectors $\boldsymbol{e}_0$ and $\boldsymbol{h}_0$ need to be real-valued in order to keep the symmetry $h_q(\omega) = -h_q^*(-\omega^*)$. The quadratic form $q(\omega)$ is a linear combination of different components of the material matrices $\boldsymbol{\epsilon}(\omega)$, $\boldsymbol{\xi}(\omega)$, $\boldsymbol{\zeta}(\omega)$, and $\boldsymbol{\mu}(\omega)$, but not all linear combinations are possible, only those corresponding to diagonal elements of the 6×6 material matrix. Note in particular that we cannot find a Herglotz function $h_q(\omega)$ involving *only* the matrices $\boldsymbol{\xi}(\omega)$ or $\boldsymbol{\zeta}(\omega)$, they are always mixed with $\boldsymbol{\epsilon}(\omega)$ or $\boldsymbol{\mu}(\omega)$. We must also take into account that for reciprocal media, the static limit of $\boldsymbol{\xi}(\omega)$ and $\boldsymbol{\zeta}(\omega)$ is zero, since the coupling between electric and magnetic fields disappears in the static limit [25, p. 36], so that

$$q(0) = \begin{pmatrix}\boldsymbol{e}_0\\ \boldsymbol{h}_0\end{pmatrix}\cdot\begin{pmatrix}\boldsymbol{\epsilon}(0) & \mathbf{0}\\ \mathbf{0} & \boldsymbol{\mu}(0)\end{pmatrix}\begin{pmatrix}\boldsymbol{e}_0\\ \boldsymbol{h}_0\end{pmatrix} = \boldsymbol{e}_0\cdot\boldsymbol{\epsilon}(0)\boldsymbol{e}_0 + \boldsymbol{h}_0\cdot\boldsymbol{\mu}(0)\boldsymbol{h}_0 \tag{4.4}$$

For instance, this means that the bound (3.7) for bi-anisotropic materials becomes

$$\max_{\omega\in\mathcal{B}}|q(\omega)-q_{\mathrm{m}}| \geq \frac{B}{1+B/2}(q_\infty - q_{\mathrm{m}})\begin{cases}1/2 & \text{lossy case}\\ 1 & \text{lossless case,}\end{cases} \tag{4.5}$$

The simplest example of a material with coupling between electric and magnetic fields is a chiral material, which is a bi-isotropic material where all material matrices are proportional to the identity matrix $\mathbf{I}$,

$$\begin{pmatrix}\boldsymbol{\epsilon}(\omega) & \boldsymbol{\xi}(\omega)\\ \boldsymbol{\zeta}(\omega) & \boldsymbol{\mu}(\omega)\end{pmatrix} = \begin{pmatrix}\epsilon(\omega)\mathbf{I} & \mathrm{i}\chi(\omega)\mathbf{I}\\ -\mathrm{i}\chi(\omega)\mathbf{I} & \mu(\omega)\mathbf{I}\end{pmatrix} \tag{4.6}$$

The quadratic form $q(\omega)$ then only contains information on $\epsilon(\omega)$ and $\mu(\omega)$,

$$q(\omega) = \begin{pmatrix}\boldsymbol{e}_0\\ \boldsymbol{h}_0\end{pmatrix}\cdot\begin{pmatrix}\epsilon(\omega)\mathbf{I} & \mathrm{i}\chi(\omega)\mathbf{I}\\ -\mathrm{i}\chi(\omega)\mathbf{I} & \mu(\omega)\mathbf{I}\end{pmatrix}\begin{pmatrix}\boldsymbol{e}_0\\ \boldsymbol{h}_0\end{pmatrix} = |\boldsymbol{e}_0|^2\epsilon(\omega) + |\boldsymbol{h}_0|^2\mu(\omega) \tag{4.7}$$

This means the sum rules in this paper can be used to bound a linear combination of $\epsilon(\omega)$ and $\mu(\omega)$, but provide no information on $\chi(\omega)$. This is due to the requirement of $\boldsymbol{e}_0$ and $\boldsymbol{h}_0$ to be real-valued vectors. The physical importance of the chirality parameter χ is that it is proportional to the rotation of the polarization direction of a linearly polarized wave as it propagates through the chiral material. Denoting the real and imaginary parts with primes as $\chi = \chi' + \mathrm{i}\chi''$, the angle of rotation is [29]

$$\phi(\omega) = \frac{\omega}{c_0}\chi'(\omega) = \frac{2\pi}{\lambda}\chi'(\omega) \tag{4.8}$$

per unit length of propagation. The following sum rule is proposed in [29]

$$\int_0^\infty \omega\chi'(\omega)\,\mathrm{d}\omega = 0 \quad \Leftrightarrow \quad \int_0^\infty \phi(\omega)\,\mathrm{d}\omega = 0 \tag{4.9}$$

i.e., the total rotation of the polarization direction for all frequencies is zero. If the material is also an insulator at zero frequency (no static conductivity), the additional sum rule

$$\int_0^\infty \omega^{-1}\chi'(\omega)\,\mathrm{d}\omega = 0 \quad \Leftrightarrow \quad \int_0^\infty \phi(\lambda)\,\mathrm{d}\lambda = 0 \tag{4.10}$$

also applies. Thus, for an insulating chiral material, the total rotation for all frequencies *and* all wavelengths is zero [29].

5 Conclusions

In conclusion, sum rules are presented that constrain the bandwidth of passive metamaterials. The bandwidth limitations on $\epsilon(\omega) \approx \epsilon_{\mathrm{m}} < \epsilon_\infty$ are expressed in either the differences between the low- and high-frequency permittivity or the plasma frequency. The corresponding expressions for permeability or refractive index are given by replacing ϵ by μ or n. The static permittivity and permeability are well defined and can be determined by homogenization techniques for heterogeneous materials; it is then well known that the effective material parameter is bounded by the parameters of the included materials [19]. This demonstrates that for instance a high static permeability cannot be created by a composite material unless one of its component materials already has a high static permeability [1]. Many proposed metamaterial designs for negative refractive index utilize only dielectrics and metal structures, and since the static permeability of some good conductors such as copper is very close to unity, the bandwidth is penalized by (3.10) and (3.14). We have also demonstrated how *a priori* information about the plasma frequency can be used to derive additional sum rules. Finally, we have shown that the sum rules can be applied to bi-anisotropic material models, but only for the diagonal elements of the 6×6 material matrix.

Acknowledgments

The support of the Swedish research council is gratefully acknowledged.

References

[1] O. Acher. Copper vs iron: Microwave magnetism in the metamaterial age. *J. Magn. Magn. Mater.*, **321**, 2093–2101, 2009.

[2] A. Alù and N. Engheta. Theory and potentials of multi-layered plasmonic covers for multi-frequency cloaking. *New Journal of Physics*, **10**, 115036, 2008.

[3] C. R. Brewitt-Taylor. Limitation on the bandwidth of artificial perfect magnetic conductor surfaces. *Microwaves, Antennas & Propagation, IET*, **1**(1), 255–260, 2007.

[4] R. M. Fano. Theoretical limitations on the broadband matching of arbitrary impedances. *Journal of the Franklin Institute*, **249**(1,2), 57–83 and 139–154, 1950.

[5] M. Gustafsson, C. Sohl, and G. Kristensson. Physical limitations on antennas of arbitrary shape. *Proc. R. Soc. A*, **463**, 2589–2607, 2007.

[6] M. Gustafsson, C. Sohl, and G. Kristensson. Illustrations of new physical bounds on linearly polarized antennas. *IEEE Trans. Antennas Propagat.*, **57**(5), 1319–1327, May 2009.

[7] M. Gustafsson. On the non-uniqueness of the electromagnetic instantaneous response. *J. Phys. A: Math. Gen.*, **36**, 1743–1758, 2003.

[8] M. Gustafsson. Sum rule for the transmission cross section of apertures in thin opaque screens. *Opt. Lett.*, **34**(13), 2003–2005, 2009.

[9] M. Gustafsson, C. Sohl, C. Larsson, and D. Sjöberg. Physical bounds on the all-spectrum transmission through periodic arrays. *EPL Europhysics Letters*, **87**(3), 34002 (6pp), 2009.

[10] J. D. Jackson. *Classical Electrodynamics*. John Wiley & Sons, New York, third edition, 1999.

[11] I. S. Kac and M. G. Kreĭn. R-functions — analytic functions mapping the upper halfplane into itself. *Amer. Math. Soc. Transl.(2)*, **103**, 1–18, 1974.

[12] A. Karlsson and G. Kristensson. Constitutive relations, dissipation and reciprocity for the Maxwell equations in the time domain. *J. Electro. Waves Applic.*, **6**(5/6), 537–551, 1992.

[13] F. W. King. *Hilbert Transforms, Volume 2*. Cambridge University Press, 2009.

[14] P. Kinsler and M. W. McCall. Causality-based criteria for a negative refractive index must be used with care. *Phys. Rev. Lett.*, **101**, 16, 2008.

[15] H.-O. Kreiss and J. Lorenz. *Initial-Boundary Value Problems and the Navier-Stokes Equations*. Academic Press, San Diego, 1989.

[16] L. D. Landau, E. M. Lifshitz, and L. P. Pitaevskiĭ. *Electrodynamics of Continuous Media*. Pergamon, Oxford, second edition, 1984.

[17] Ø. Lind-Johansen, K. Seip, and J. Skaar. The perfect lens on a finite bandwidth. *J. Math. Phys.*, **50**, 012908, 2009.

[18] T. G. Mackay and A. Lakhtakia. Comment on"Criterion for Negative Refraction with Low Optical Losses from a Fundamental Principle of Causality". *Phys. Rev. Lett.*, **99**(18), 189701, 2007.

[19] G. W. Milton. *The Theory of Composites*. Cambridge University Press, Cambridge, U.K., 2002.

[20] B. Nistad and J. Skaar. Causality and electromagnetic properties of active media. *Phys. Rev. E*, **78**(3), 2008.

[21] H. M. Nussenzveig. *Causality and dispersion relations*. Academic Press, London, 1972.

[22] J. Ramprecht and D. Sjöberg. Biased magnetic materials in RAM applications. *Progress in Electromagnetics Research*, **75**, 85–117, 2007.

[23] K. N. Rozanov. Ultimate thickness to bandwidth ratio of radar absorbers. *IEEE Trans. Antennas Propagat.*, **48**(8), 1230–1234, August 2000.

[24] D. Schurig, J. J. Mock, B. J. Justice, S. A. Cummer, J. B. Pendry, A. F. Starr, and D. R. Smith. Metamaterial electromagnetic cloak at microwave frequencies. *Science*, **314**(5801), 977–980, November 2006.

[25] A. Serdyukov, I. Semchenko, S. Tretyakov, and A. Sihvola. *Electromagnetics of Bi-Anisotropic Materials: Theory and Applications*. Gordon and Breach Science Publishers, Amsterdam, 2001.

[26] M. G. Silveirinha and N. Engheta. Theory of supercoupling, squeezing wave energy, and field confinement in narrow channels and tight bends using ε near-zero metamaterials. *Phys. Rev. B*, **76**(24), 245109, 2007.

[27] J. Skaar and K. Seip. Bounds for the refractive indices of metamaterials. *J. Phys. D: Applied Phys.*, **39**(6), 1226, 2006.

[28] D. R. Smith, J. B. Pendry, and M. C. K. Wiltshire. Metamaterials and negative refractive index. *Science*, **305**(5685), 788–792, 2004.

[29] D. Y. Smith. Superconvergence and sum rules for the optical constants: Natural and magneto-optical activity. *Phys. Rev. B*, **13**(12), 5303–5315, 1976.

[30] C. Sohl, M. Gustafsson, and G. Kristensson. Physical limitations on broadband scattering by heterogeneous obstacles. *J. Phys. A: Math. Theor.*, **40**, 11165–11182, 2007.

[31] C. Sohl, M. Gustafsson, and G. Kristensson. Physical limitations on metamaterials: Restrictions on scattering and absorption over a frequency interval. *J. Phys. D: Applied Phys.*, **40**, 7146–7151, 2007.

[32] M. I. Stockman. Criterion for negative refraction with low optical losses from a fundamental principle of causality. *Phys. Rev. Lett.*, **98**(17), 177404, 2007.

[33] W. H. Wee and J. B. Pendry. Shrinking optical devices. *New Journal of Physics*, **11**, 073033, 2009.

[34] A. H. Zemanian. *Distribution theory and transform analysis: an introduction to generalized functions, with applications*. Dover Publications, New York, 1987.